DE GRUYTER

Chemical Papers 70 (11) 1431–1438 (2016)
DOI: 10.1515/chempap-2016-0079

ORIGINAL PAPER

Fluorescence-enhanced optical sensor for detection of Al^{3+} in water based on functionalised nanoporous silica type SBA-15

[a]Mehdi Karimi, [a,b]Alireza Badieia*, [c]Ghodsi Mohammadi Ziarani

[a]*School of Chemistry, College of Science, University of Tehran, 14155-6455 Tehran, Iran*

[b]*Nanobiomedicine Center of Excellence, Nanoscience and Nanotechnology Research Center, University of Tehran, 14155-3476 Tehran, Iran*

[c]*Department of Chemistry, Faculty of Science, Alzahra University, 1993893973 Tehran, Iran*

Received 2 October 2015; Revised 30 January 2016; Accepted 17 March 2016

An organic–inorganic hybrid optical sensor (PQ-SBA-15) was designed and prepared through functionalisation of the SBA-15 surface with 3-piperazinepropyltriethoxysilane followed by covalently attaching 8-hydroxyquinoline. Characterisation techniques, including FT-IR, thermal gravimetric, N_2 adsorption-desorption and X-ray powder diffraction analyses, showed that the organic moieties were successfully grafted onto the surface of SBA-15 without the SBA-15 structure collapsing. The evaluation of the sensing ability of PQ-SBA-15 using fluorescence spectroscopy revealed that the PQ-SBA-15 was a selective fluorescence enhancement-based optical sensor for Al^{3+} in water in the presence of a wide range of metal cations including Na^+, Mg^{2+}, K^+, Ca^{2+}, Cr^{3+}, Mn^{2+}, Fe^{3+}, Co^{2+}, Ni^{2+}, Cu^{2+}, Zn^{2+}, Cd^{2+}, Hg^{2+} and Pb^{2+} with a limit of detection of 8.8×10^{-7} M. In addition, good linearity was observed between the fluorescence intensity and the concentration of Al^{3+}.

Keywords: fluorescence, nanoporous silica material, SBA-15, optical sensor, Al^{3+}

Introduction

Aluminium is the third most abundant metal in the Earth's crust and is widely used in the making of cans, wrapping foil, household utensils and Al-contained medicines. It has also found numerous applications in vehicles, aircraft and the construction industries (Robinson, 2003). However, an excessive amount of Al^{3+} may represent a serious hazard for the central nervous system, especially conducive to the appearance of symptoms of Alzheimer's and Parkinson's diseases (Exley, 1999; Flaten, 1990; McLachlan, 1995). It is also a major factor impeding plant production on acidic soils (Delhaize & Ryan, 1995); therefore, the ability to detect Al^{3+} is an important task for maintaining good human health and good environmental conditions.

Fluorescent sensors have recently attracted a great deal of attention in the detection of Al^{3+} (Das et al., 2013) due to their advantages of simple operation, selectivity, sensitivity and real-time monitoring. However, the optimal working conditions for most of the reported sensors for the detection of Al^{3+} entailed the use of organic solvents (Azadbakht et al., 2013; Chang et al., 2014; Dong et al., 2012; Li et al., 2014; Othman et al., 2007; Xu et al., 2014; Zhao et al., 2006), which limits the practical application of these sensors to function directly in water. Hence, designing fluorescent sensors capable of the detection of Al^{3+} in aqueous media is highly desirable.

As an emerging type of fluorescent sensors, organic-inorganic hybrid optical sensors have recently attracted attention for the detection of various ions (Han, 2009). These sensors are constructed based on

*Corresponding author, e-mail: abadiei@khayam.ut.ac.ir

the immobilisation of organic fluorophores onto the surface of inorganic matrices. Among various inorganic matrices, the nanoporous silica material type SBA-15 has become an ideal candidate for the fabrication of hybrid optical sensors due to its high specific surface area, uniform channels, large pore diameter, hydrothermal stability and biocompatibility (Balaji et al., 2005; Comes et al., 2005; Descalzo et al., 2002; Gao et al., 2006; Meng et al., 2011; Métivier, 2005; Wang et al., 2010; Xu, 2013; Yadavi, 2013a, 2013b; Zarabadi-Poor, 2013). In addition, SBA-15 is non-fluorescent and optically transparent in the visible range. Moreover, the covalent grafting of organic entities into the SBA-15 channels renders the optical sensor more durable than the molecular chemosensors because organic entities are prevented from leaching into the solution.

8-Hydroxyquinoline (8-HQ) and its derivatives are important chelators and sensors for many metal ions because they can serve as both metal-binding site and fluorophore (Descalzo et al., 2002; Xu et al., 2012; Zhou et al., 2012), especially for Al^{3+} (Badiei, 2011; Goswami, 2013; Jiang et al., 2011; Maity & Govindaraju, 2012; Zhao et al., 2006). Accordingly, it was presumed that the tendency of 8-HQ for binding to Al^{3+} could be exploited to prepare an SBA-15-based optical sensor for the detection of Al^{3+}. The present study-group previously reported on the use of nanoporous silica material type SBA-15 for the preparation of optical sensors (Karimi, 2015a, 2015b). These optical sensors, as reported, were capable of selectively detecting Fe^{3+} using 1-aminonaphthalene as fluorophore and Pb^{2+} and I^- using 8-HQ as fluorophore. In the continuing investigation into the use of nanoporous silica material, especially SBA-15, in optical sensors, an optical sensor based on SBA-15 as the inorganic host material and 8-HQ as an organic fluorescent guest is reported for the detection of Al^{3+} in water. A comparison of the results of the current work with the previous study (Karimi, 2015a) reveals that changing the attachment mode of 8-HQ onto the SBA-15 surface resulted in a completely different sensing behaviour. To the best of our knowledge, the sensing of Al^{3+} with a nanoporous silica-based optical sensor has not previously been reported.

Experimental

8-HQ (assay 99 %), hydrochloric acid 35 % (ACS grade) and Pluronic P_{123} ($EO_{20}PO_{70}EO_{20}$, M_w = ca. 5800) were purchased from Sigma–Aldrich (USA) and 3-piperazinepropyltriehtoxysilane (PPTES; purity 99 %) was purchased from Shondong wanda company (China). All the solvents including toluene (purity 99 %), CH_2Cl_2 (grade 99.8 %), ethanol (99.9 %) were obtained from Merck (Germany). All the above materials were used without further purification. Deionised water was used in all the procedures.

Synthesis of 5-chloromethyl-8-hydroxyquinoline

To synthesise 5-chloromethyl-8-hydroxyquinoline, following a procedure proposed by Kolobielski (1966), a mixture of 8-HQ (10 g, 0.07 mol), HCl (25 mL, 35 %) and formaldehyde (25 mL, 37 %) was prepared and stirred under an HCl gas flow for about 5 h at 0 °C. The resultant yellow powder was then washed with diethyl ether and dried overnight (melting point 280 °C).

Synthesis of P-SBA-15

SBA-15 was synthesised following a procedure suggested by Bahrami et al. (2014): dried SBA-15 (1 g) was dispersed in toluene (100 mL) by stirring for 0.5 h. Next, PPTES (5 mmol) was added and the mixture was refluxed for 6 h under an argon atmosphere. The piperazine-functionalised SBA-15 (P-SBA-15) so obtained was filtered, washed with an excessive amount of toluene and dried overnight at 80 °C in an oven.

Synthesis of PQ-SBA-15

PQ-SBA-15 was synthesised as follows: P-SBA-15 (1 g) was dispersed in 50 mL of dried CH_2Cl_2 by stirring for 0.5 h. Next, Et_3N (5 mmol) and 5-chloromethyl-8-hydroxyquinoline (5 mmol) were added to the homogeneous mixture and it was refluxed for 24 h. The final product was filtered, washed with an excessive amount of CH_2Cl_2 and ethanol and dried overnight at 80 °C in an oven. The overall synthesis procedure is depicted in Fig. 1.

Instruments and spectroscopic measurements

Low-angle X-ray scattering measurements were performed on an X'Pert Pro MPD diffractometer (PANalytical, the Netherlands) using CuK_α radiation (λ = 1.5418 Å). N_2 adsorption–desorption isotherms were obtained using a BELSORP-miniII instrument (Microtrac, Japan) at liquid nitrogen temperature (–196 °C). All samples were degassed at 100 °C prior to performing the measurements. The Brunauer–Emmet–Teller (BET) and Barrett–Joyner–Halenda (BJH) equations were applied to the sorption data using BELSORP analysis software (Microtrac) to calculate the physical properties of the materials such as specific surface area, pore diameter, pore volume and pore size distribution. The Fourier transform infrared (FT-IR) spectra of samples were recorded on a RAYLEIGH WQF-510A apparatus (BRAIC, China). Transmission electron microscopy (TEM) was performed on a Zeiss EM900 instrument (Germany) at an accelerating voltage of 80 kV. The samples were dispersed in ethanol using an ultrasonic bath and a drop of the ethanol mixture was placed on a lacey carbon-coated copper grid for analysis. Thermogravimetric analysis (TGA) was carried out us-

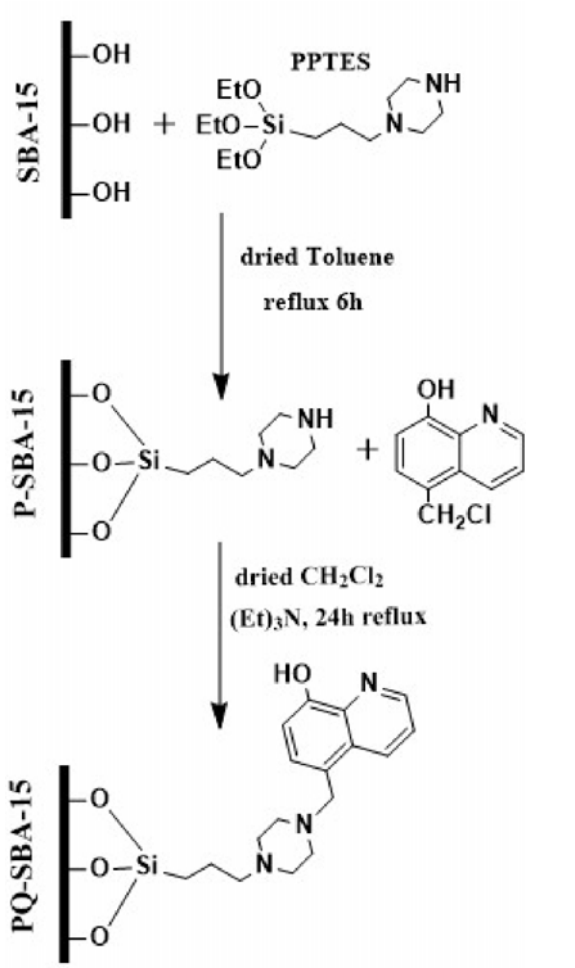

Fig. 1. Synthesis procedure of PQ-SBA-15.

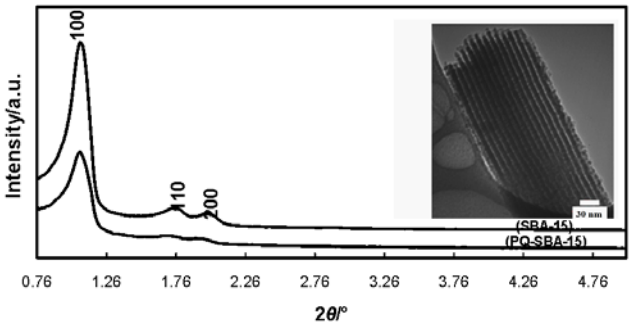

Fig. 2. XRD patterns of SBA-15 and PQ-SBA-15 (inset: TEM image of SBA-15).

ing a TGA Q50 V6.3 Build 189 instrument (TA instruments, USA) in an air atmosphere from ambient temperature to 800 °C with a ramp rate of 20 °C min^{-1} in air atmosphere. Fluorescence spectra were recorded on an Agilent G980A instrument (Agilent, USA).

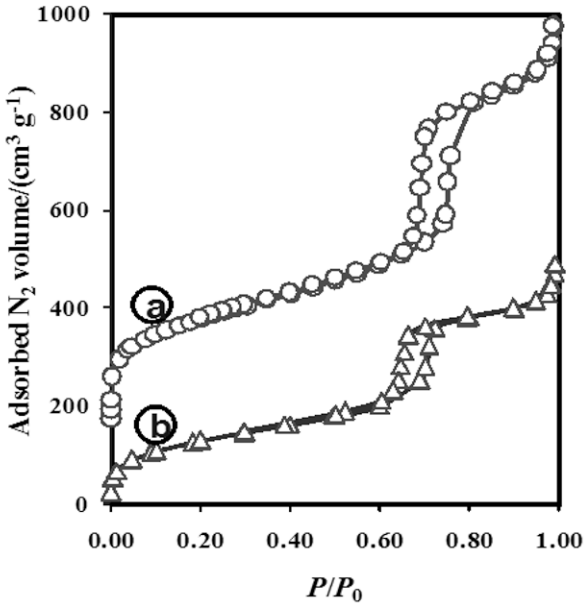

Fig. 3. N2 adsorption-desorption isotherms of: a) SBA-15 and; b) PQ-SBA-15.

Results and discussion

Fig. 2 shows the low-angle X-ray diffraction patterns of SBA-15 and PQ-SBA-15. In general, the SBA-15 material exhibits three characteristic diffractions: a single intensive diffraction near $2\theta = 1°$ indexed to the (100) plane and two weak peaks near $2\theta = 2°$ indexed to the (110) and (200) planes (Sun et al., 2008). The presence of these three diffractions implies that the structure possesses a long-range periodic order and a two-dimensional hexagonal (p6mm) mesostructure. Both samples exhibited the above diffractions, indicating that the original structure of SBA-15 was preserved after the functionalisation steps. However, the decrease in the intensity of the (100), (110) and (200) diffractions in PQ-SBA-15 may be due to the reduction in scattered X-ray radiation resulting from covering the surface with the attachments of the organic moieties (Li & Yan, 2009). The Fig. 2 inset shows the TEM image of SBA-15 which displays two-dimensional channels throughout the particle with a pore diameter of approximately 6 nm.

The N_2 adsorption–desorption isotherms of SBA-15 and PQ-SBA-15 are shown in Fig. 3. SBA-15 exhibits a type IV standard IUPAC isotherm, corresponding to the mesoporous materials (Sing et al., 1982). In addition, the presence of the H1 type hysteresis loop and sharp capillary condensation steps at P/P_0 of 0.6–0.8 are characteristic of a highly ordered structure. A similar isotherm, with a lower level of gas adsorption as well as lower height of the hysteresis loop, was observed for PQ-SBA-15, indicating that the porosity of the original SBA-15 was preserved and the pores in PQ-SBA-15 were not blocked during

Table 1. Textural parameters of SBA-15 and PQ-SBA-15

Sample	$S_{BET}/(m^2\ g^{-1})$	d_P/nm	$V_P/(cm^3\ g^{-1})$
SBA-15	788	6.5	1.28
PQ-SBA-15	458	5.4	0.73

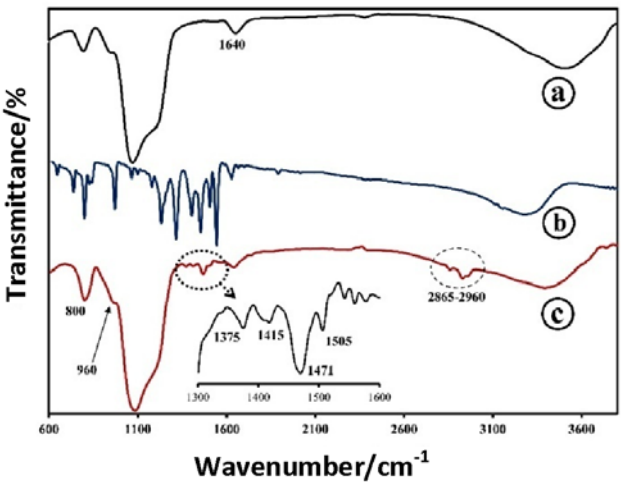

Fig. 4. FT-IR spectra of: a) SBA-15, (b) 8-HQ and c) PQ-SBA-15.

the modification steps, hence the channels remained open to diffuse ions into them. The lower level of gas adsorption confirmed that the organic moieties were successfully incorporated into the surface, causing a significant decrease in pore volume and specific surface area in PQ-SBA-15. Specific surface area (S_{BET}), average pore diameter (d_p) and average pore volume (V_p) of SBA-15 and PQ-SBA-15 are given in Table 1. A decrease in all three parameters was observed in the functionalised PQ-SBA-15 in comparison with the original SBA-15.

Fig. 4 shows the FT-IR spectra of SBA-15 and PQ-SBA-15. The bands located at around 800 cm^{-1}, 960 cm^{-1}, 1100 cm^{-1} and 3434 cm^{-1} in the spectra of SBA-15 and PQ-SBA-15 were assigned to the symmetric stretching vibrations of Si—O, the symmetric stretching vibration of Si—OH, the asymmetric stretching vibrations of Si—O—Si vibrations, and the stretching vibrations of the OH groups, respectively. The band at around 1640 cm^{-1} is attributed to the physically absorbed water molecules. The bands related to the stretching vibrations of the tertiary aliphatic amines normally occur at around 1150–1210 cm^{-1} where they overlapped with the intense Si—O—Si band, hence they may not be observed. The bands at around 1415 cm^{-1} and within the 2865–2960 cm^{-1} range were related to the stretching vibrations of the $-CH_2-$ groups of the propyl chain. The band corresponding to the phenolic OH appeared at

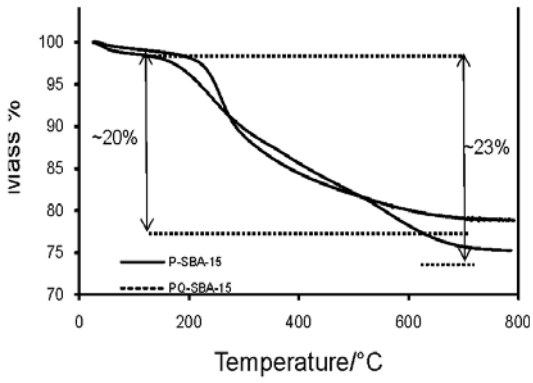

Fig. 5. TGA curves of P-SBA-15 and PQ-SBA-15.

1375 cm^{-1} and the bands corresponding to the aromatic C═C and C═N ring vibrations of the attached 8-HQ group appeared at 1471 cm^{-1} and at 1505 cm^{-1} (Lan & Yang., 1994). Hence, the FT-IR results confirmed the successful attachment of the organic moieties onto the surface of SBA-15.

The amount of 8-HQ attached to the surface of SBA-15 was estimated by the TGA curves of P-SBA-15 and PQ-SBA-15 in Fig. 5. In both cases, the mass loss between 40–150 ℃ was due to the elimination of the physisorbed water molecules. Organic moieties were eliminated in the range of 150–700 ℃ and, finally, the mass loss above 700 ℃ was due to the dehydroxylation of the Si—OH groups from the SBA-15 framework (Zarabadi-Poor et al., 2013). The mass loss percentages of the eliminated organic moieties were estimated to be ≈ 20 % for P-SBA-15 and 23 % PQ-SBA-15. Next, the 3 % difference between the two figures was assigned to the amount of grafted 8-HQ. Accordingly, the amount of the attached 8-HQ was estimated to be approximately 0.19 mmol g^{-1} in the PQ-SBA-15 sample.

To evaluate the sensing ability, PQ-SBA-15 was dispersed in water (0.4 g L^{-1}) and the changes in the fluorescence emission of the aqueous suspension of PQ-SBA-15 in the absence and presence of a wide range of metal cations, including Na^+, Mg^{2+}, Al^{3+}, K^+, Ca^{2+}, Cr^{3+}, Mn^{2+}, Fe^{3+}, Co^{2+}, Ni^{2+}, Cu^{2+}, Zn^{2+}, Cd^{2+}, Hg^{2+} and Pb^{2+} (1×10^{-2} M), at pH = 7 were recorded. The settings applied throughout the fluorescence experiments were: excitation wavelength of 360 nm, excitation and emission slit numbers of 5. In each test, 100 μL of cations solution was added to 3 mL of the suspension of PQ-SBA-15 and the spectrum was recorded after 1 min to ensure that stability in emission intensity was achieved. It should be noted that, due to the protective effect of the SBA-15 structure in environments with various pH values, the measurements were carried out in an unbuffered solution (Zarabadi-Poor et al., 2013). Fig. 6 illustrates the detailed fluorescence responses of PQ-SBA-15 toward the cations. The PQ-SBA-15 reference

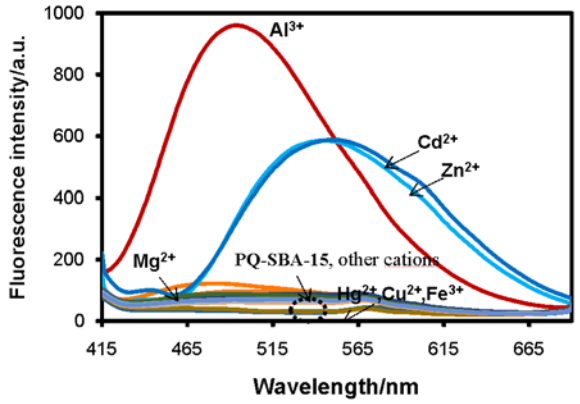

Fig. 6. Fluorescence response of aqueous suspension of PQ-SBA-15 (0.4 g L^{-1}) upon addition of different cations including Na^+, Mg^{2+}, Al^{3+}, K^+, Ca^{2+}, Cr^{3+}, Mn^{2+}, Fe^{3+}, Co^{2+}, Cu^{2+}, Zn^{2+}, Cd^{2+}, Hg^{2+} and Pb^{2+} (100 μL, 1×10^{-2} mol L^{-1}); $\lambda_{ex} = 360$ nm and $\lambda_{em} = 485$ nm.

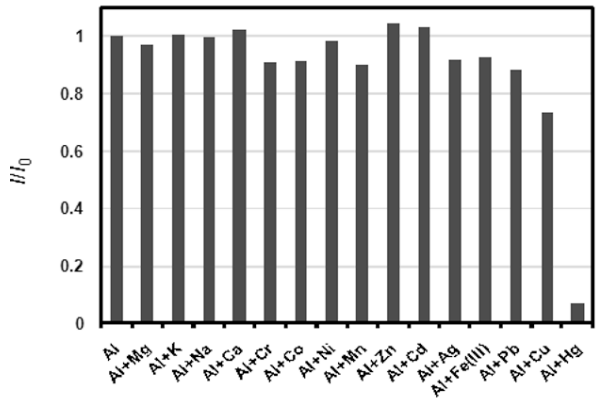

Fig. 8. Interference from other cations in water: PQ-SBA-15 (0.4 g L^{-1}) + Al^{3+} (20 μL, 1×10^{-2} mol L^{-1}) + M^{n+} (80 μL, 1×10^{-2} mol L^{-1}) where $M^{n+} = Na^+$, Mg^{2+}, K^+, Ca^{2+}, Cr^{3+}, Mn^{2+}, Fe^{3+}, Co^{2+}, Ni^{2+}, Cu^{2+}, Zn^{2+}, Cd^{2+}, Hg^{2+} and Pb^{2+}; $\lambda_{ex} = 360$ nm and $\lambda_{em} = 485$ nm.

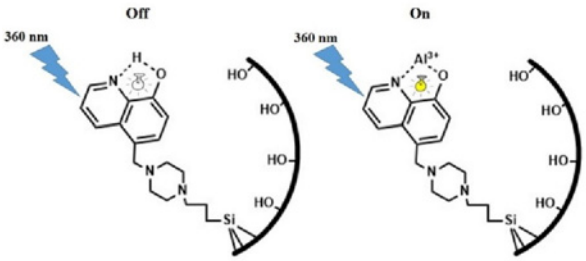

Fig. 7. On-off states of fluorescence emission.

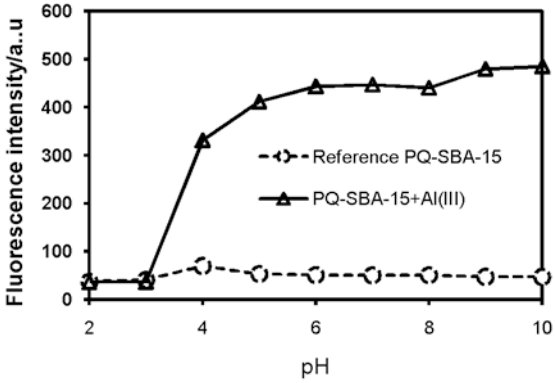

Fig. 9. Fluorescence intensity of aqueous suspension of PQ-SBA-15 prior to and after addition of Al^{3+} at various pH values; $\lambda_{ex} = 360$ nm and $\lambda_{em} = 485$ nm.

exhibited a very week fluorescence emission and exhibited a negligible change in fluorescence intensity upon the addition of Na^+, Mg^{2+}, K^+, Ca^{2+}, Cr^{3+}, Mn^{2+}, Fe^{3+}, Co^{2+}, Ni^{2+}, Cu^{2+}, Hg^{2+} and Pb^{2+}. The remarkable fluorescence enhancement (approximately 10-fold in comparison with free PQ-SBA-15) was observed in the presence of Al^{3+} with the maximum emission wavelength at 485 nm. Also, a fluorescence enhancement was observed upon the addition of Cd^{2+} and Zn^{2+} which were distinguishable from Al^{3+} with a red-shift about 70 nm in the maximum emission wavelength in comparison with Al^{3+}. 8-HQ is known to be a weak fluorescent molecule due to the excited-state intramolecular proton transfer process from oxygen to nitrogen (Hao et al., 2011) and the photo-induced electron transfer (PET) involving the lone pair of tertiary nitrogen (Bardez, 1997). A mechanism for the fluorescence enhancement by Al^{3+} is proposed in Fig. 7. Upon the chelation of 8-HQ with Al^{3+}, the quenching mechanisms are blocked and the 8-HQ subsequently emits an intensive fluorescence emission, i.e. the chelating-enhanced fluorescence (CHEF) effect occurred.

To examine the selectivity for Al^{3+}, the fluorescence response of the aqueous suspension of PQ-SBA-15 containing Al^{3+} in competition with other cations as interfering agents was also recorded and the results are depicted in Fig. 8. In these experiments, 3 mL of the aqueous suspension of PQ-SBA-15 was added to the mixture of 20 μL of Al^{3+} + 80 μL of M^{n+}. With the exception of Hg^{2+} which significantly quenched the fluorescence emission, the other cations had a minor or negligible effect on the fluorescence spectrum of the PQ-SBA-15[Al^{3+}] system. Thus, PQ-SBA-15 can be considered as a selective fluorescence enhancement-based optical sensor for the direct detection of Al^{3+} in water.

In addition, to evaluate the effect of pH on the capacity of PQ-SBA-15 for the detection of Al^{3+}, the fluorescence spectra of PQ-SBA-15 with and without Al^{3+} (50 μL, 1×10^{-2} mol L^{-1}), at different pH values ranging from 2 to 10 were recorded; the results are provided in Fig. 9. The pH of the test

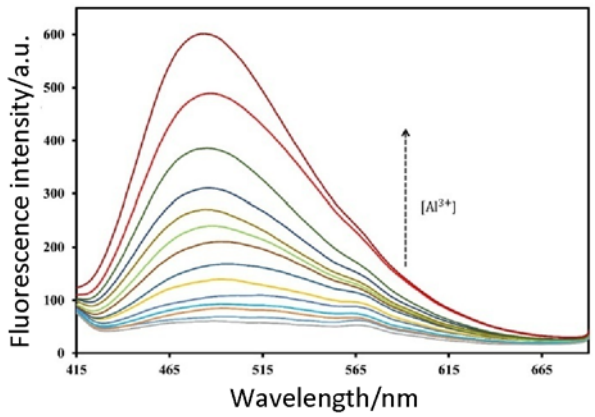

Fig. 10. Fluorescence spectra of aqueous suspension of PQ-SBA-15 (0.4 g L^{-1}) after addition of increasing amount of Al^{3+} within the range of 10^{-5}–10^{-6} mol L^{-1}; λ_{ex} = 360 nm and λ_{em} = 485 nm.

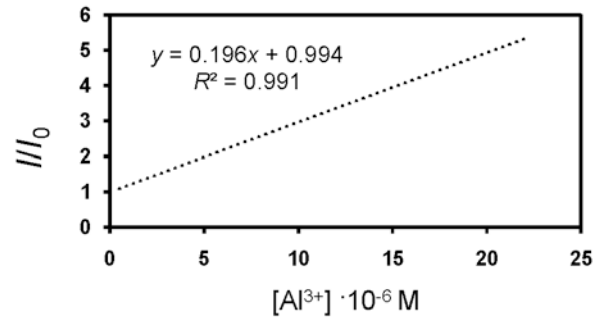

Fig. 11. Plot of normalised fluorescence response I/I_0 of aqueous suspension of PQ-SBA-15 (0.4 g L^{-1}) versus concentration of Al^{3+}; λ_{ex} = 360 nm and λ_{em} = 485 nm.

solutions was adjusted by HCl and NaOH solutions. The fluorescence intensity of the aqueous suspension of PQ-SBA-15 without Al^{3+} is independent of the pH values, indicating that the quenching mechanism of 8-HQ remained constant at various pH values. On the other hand, the fluorescence intensity was completely quenched in an acidic solution even in the presence of Al^{3+} (50 μL, 1 × 10^{-2} mol L^{-1}); however, the fluorescence intensity in the presence of Al^{3+} was gradually enhanced with an increase in pH values. Hence, PQ-SBA-15 is applicable to the detection of Al^{3+} in aqueous media at pH values ranging from 5 to 10.

A fluorescence titration experiment of the aqueous suspension of PQ-SBA-15 (0.4 g L^{-1}) in the presence Al^{3+} in the concentration range from 0 μL to 60 μL (1 × 10^{-2} mol L^{-1}) was carried out. Fig. 10 shows that, with an increase in the concentration of Al^{3+}, the fluorescence intensity progressively increased.

Based on the fluorescence titration data, the plot of I/I_0 vs. the concentration of Al^{3+} was constructed, as provided in Fig. 11, demonstrating a good linear relationship between the concentration of Al^{3+} and the fluorescence intensity of the aqueous suspension of PQ-SBA-15 with a linearly dependent coefficient (R^2) of 0.9919. However, it should be noted that the linearity was observed at low concentrations of the ion within the range of 10^{-6}–10^{-5} M and the deviation from linear behaviour was observed in higher concentrations, hence the linearity plot was obtained for this linear range. The limit of detection of Al^{3+} was calculated using the following equation:

$$D_L = \frac{3S_D}{m} \quad (1)$$

where D_L is the smallest amount that can be detected, S_D is the standard deviation of the blank solution measured 6 times, and m is the plot slope of the fluorescence intensity versus [Al^{3+}]. In this case, S_D and m were 3.5 and 11.8 × 10^6, respectively. Then D_L was calculated to be 8.8 × 10^{-7} mol L^{-1}.

Conclusions

An organic–inorganic hybrid optical sensor (PQ-SBA-15) for detecting Al^{3+} ions in water was prepared by covalently immobilising 8-HQ as a fluorophore and binding site onto the surface of SBA-15 using the post-grafting method. The characterisation of the materials thus prepared using FT-IR spectroscopy, thermogravimetric analysis (TGA), N_2 adsorption-desorption and X-ray powder diffraction analysis confirmed that the 8-HQ groups were successfully attached onto the surface of SBA-15 without collapsing or altering the original SBA-15 mesostructure. As a fluorescence enhancement-based optical sensor, PQ-SBA-15 was able to directly detect Al^{3+} in water across the wide range of metal cations present with approximately a 10-fold increase in fluorescence intensity resulting from the CHEF effect. This sensor exhibited selectivity for Al^{3+} in the presence of other cations (except for Hg^{2+}) as interfering ions, even with the presence of a higher concentration of those ions. A good linearity between the fluorescence intensity of PQ-SBA-15 and the concentration of Al^{3+} was obtained with a limit of detection of 8.8 × 10^{-7} M.

Acknowledgements. The authors wish to thank the research council of the University of Tehran for the financial support received.

References

Azadbakht, R., Almasi, T., Keypour, H., & Rezaeivala, M. (2013). A new asymmetric Schiff base system as fluorescent chemosensor for Al^{3+} ion. *Inorganic Chemistry Communications*, *33*, 63–67. DOI: 10.1016/j.inoche.2013.03.014.

Badiei, A., Goldooz, H., Ziarani, G. M., & Abbasi, A. (2011). One pot synthesis of functionalized SBA-15 by using an 8-hydroxyquinoline-5-sulfonamide-modified organosilane as precursor. *Journal of Colloid and Interface Science*, *357*, 63–69. DOI: 10.1016/j.jcis.2011.01.049.

Bahrami, Z., Badiei, A., & Atyabi, F. (2014). Surface functionalization of SBA-15 nanorods for anticancer drug delivery.

Chemical Engineering Research and Design, *92*, 1296–1303. DOI: 10.1016/j.cherd.2013.11.007.

Balaji, T., Sasidharan, M., & Matsunaga, H. (2005). Optical sensor for the visual detection of mercury using mesoporous silica anchoring porphyrin moiety. *Analyst*, *130*, 1162–1167. DOI: 10.1039/b503261j.

Bardez, E., Devol, I., Larrey, B., & Valeur, B. (1997). Excited-state processes in 8-hydroxyquinoline: photoinduced tautomerization and solvation effects. *The Journal of Physical Chemistry B*, *101*, 7786–7793. DOI: 10.1021/jp971293u.

Chang, Y., Hung, P., Wan, C., & Wu, A. (2014). A highly selective fluorescence turn-on and reversible sensor for Al^{3+} ion. *Inorganic Chemistry Communications*, *39*, 122–125. DOI: 10.1016/j.inoche.2013.11.019.

Comes, M., Rodríguez-López, G., Dolores Marcos, M., Martínez-Máñez, R., Sancenón, F., Soto, J., Beltrán, D. (2005). Host solids containing nanoscale anion-binding pockets and their use in selective sensing displacement assays. *Angewandte Chemie International Edition*, *117*, 2978–2982. DOI: 10.1002/anie.200461511.

Das, S., Dutta, M., & Das, D. (2013). Fluorescent probes for selective determination of trace level Al^{3+}: recent developments and future prospects. *Analytical Methods*, *5*, 6262–6285. DOI: 10.1039/c3ay40982a.

Delhaize, E., & Ryan, P. R. (1995). Aluminum toxicity and tolerance in plants. *Plant Physiology*, *107* , 315–321.

Descalzo, A. B., Jimenez, D., Marcos, M. D., Martínez-Máñez, R., Soto, J., El Haskouri, J., & Borrachero, M. V. (2002). A new approach to chemosensors for anions using MCM-41 grafted with amino groups. *Advanced Materials*, *14*, 966–969. DOI: 10.1002/1521-4095(20020705)14:13/14< 966::AID-ADMA966> 3.0.CO;2-D.

Dong, M., Dong, Y., Ma, T., Wang, Y., & Peng, Y. (2012). A highly selective fluorescence-enhanced chemosensor for Al^{3+} in aqueous solution based on a hybrid ligand from BINOL scaffold and β-amino alcohol. *Inorganica Chimica Acta*, *381*, 137–142. DOI: 10.1016/j.ica.2011.08.043.

Exley, C. (1999). A molecular mechanism of aluminium-induced Alzheimer's disease? *Journal of Inorganic Biochemistry*, *76*, 133–140. DOI: 10.1016/s0162-0134(99)00125-7.

Flaten, T. P. (1990). Geographical associations between aluminium in drinking water and death rates with dementia (including Alzheimer's disease), Parkinson's disease and amyotrophic lateral sclerosis in Norway. *Environmental Geochemistry and Health*, *12*, 152–167. DOI: 10.1007/bf01734064.

Gao, L., Wang, Y., Wang, J., Huang, L., Shi, L., Fan, X., Zou, Z., Yu, T., Zhu, M., & Li, Z. (2006). A novel Zn^{II}-sensitive fluorescent chemosensor assembled within aminopropyl-functionalized mesoporous SBA-15. *Inorganic Chemistry*, *45*, 6844–6850. DOI: 10.1021/ic0516562.

Goswami, S., Aich, K., Das, A. K., Manna, A., & Das, S. (2013). A naphthalimide–quinoline based probe for selective, fluorescence ratiometric sensing of trivalent ions. *RSC Advances*, *3*, 2412–2416. DOI: 10.1039/c2ra22624c.

Han, W. S., Lee, H. Y., Jung, S. H., Lee, S. J., & Jung, J. H. (2009). Silica-based chromogenic and fluorogenic hybrid chemosensor materials. *Chemical Society Reviews*, *38*, 1904–1915. DOI: 10.1039/b818893a.

Hao, E., Meng, T., Zhang, M., Pang, W., Zhou, Y., & Jiao, L. (2011). Solvent dependent fluorescent properties of a 1,2,3-triazole linked 8-hydroxyquinoline chemosensor: Tunable detection from zinc(II) to iron(III) in the CH_3CN/H_2O system. *The Journal of Physical Chemistry A*, *115*, 8234–8241. DOI: 10.1021/jp202700s.

Jiang, X., Wang, B., Yang, Z., Liu, Y., Li, T., & Liu, Z. (2011). 8-Hydroxyquinoline-5-carbaldehyde Schiff-base as a highly selective and sensitive Al^{3+} sensor in weak acid aqueous medium. *Inorganic Chemistry Communications*, *14*, 1224–1227. DOI: 10.1016/j.inoche.2011.04.027.

Karimi, M., Badiei, A., & Ziarani, G. M. (2015a). A single hybrid optical sensor based on nanoporous silica type SBA-15 for detection of Pb^{2+} and I^- in aqueous media. *RSC Advances*, *5*, 36530–36539. DOI: 10.1039/c5ra02692j.

Karimi, M., Badiei, A., & Ziarani, G. M. (2015b). A novel naphthalene-immobilized nanoporous SBA-15 as a highly selective optical sensor for detection of Fe^{3+} in water. *Journal of Fluorescence*, *25*, 1297–1302. DOI: 10.1007/s10895-015-1617-y.

Kolobielski, M. (1966). The synthesis of substituted 8-quinolinols. *Journal of Heterocyclic Chemistry*, *3*, 275–277. DOI: 10.1002/jhet.5570030308.

Lan, C., & Yang, M. (1994). Synthesis, properties and applications of silica-immobilized 8-quinolinol: Part 1. Characterization of silica-immobilized 8-quinolinol synthesized via a Mannich reaction. *Analytica chimica acta*, *287*, 101–109. DOI: 10.1016/0003-2670(94)85107-7.

Li, Y., & Yan, B. (2009). Lanthanide (Eu^{3+}, Tb^{3+})/β-diketone modified mesoporous SBA-15/organic polymer hybrids: chemically bonded construction, physical characterization, and photophysical properties. *Inorganic Chemistry*, *48*, 8276–8285. DOI: 10.1021/ic900971h.

Li, T., Fang, R., Wang, B., Shao, Y., Liu, J., Zhang, S., & Yang, Z. (2014). A simple coumarin as a turn-on fluorescence sensor for Al(III) ions. *Dalton Transactions*, *43*, 2741–2743. DOI: 10.1039/c3dt52414k.

Maity, D., & Govindaraju, T. (2012). A differentially selective sensor with fluorescence turn-on response to Zn^{2+} and dual-mode ratiometric response to Al^{3+} in aqueous media. *Chemical Communications*, *48*, 1039–1041. DOI: 10.1039/c1cc16064h.

McLachlan, D. R. C. (1995). Aluminium and the risk for Alzheimer's disease. *Environmetrics*, *6*, 233–275. DOI: 10.1002/env.3170060303.

Meng, Q., Zhang, X., He, C., Zhou, P., Su, W., & Duan, C. (2011). A hybrid mesoporous material functionalized by 1,8-naphthalimide-base receptor and the application as chemosensor and absorbent for Hg^{2+} in water. *Talanta*, *84*, 53–59. DOI: 10.1016/j.talanta.2010.12.008.

Métivier, R., Leray, I., Lebeau, B., & Valeur, B. (2005). A mesoporous silica functionalized by a covalently bound calixarene-based fluoroionophore for selective optical sensing of mercury(II) in water. *Journal of Materials Chemistry*, *15*, 2965–2973. DOI: 10.1039/b501897h.

Othman, A. B., Lee, J. W., Huh, Y., Abidi, R., Kim, J., & Vicens, J. (2007). A novel pyrenyl-appended tricalix[4]arene for fluorescence-sensing of Al(III). *Tetrahedron*, *63*, 10793–10800. DOI: 10.1016/j.tet.2007.06.120.

Robinson, G. H. (2003). Aluminum. *Chemical & Engineering News Archive*, *81*, 54. DOI: 10.1021/cen-v081n036.p054.

Sing, K. S. W., Everett, D. H., Haul, R. A. W., Moscou, L., Pierotti, R. A., Rouquerol, J., & Siemieniewska, T. (1982). Reporting physisorption data for gas/solid systems. In E. Knözinger, & Weltkamp, S. (Eds.), *Handbook of heterogeneous catalysis*, (Vol. *54*, pp. 2201–2218). New Yourk, NY, USA: Wiley-VCH. DOI: 10.1002/9783527610044.hetcat0065.

Sun, L., Zhang, H., Yu, J., Yu, S., Peng, C., Dang, S., Guo, X., & Feng, J. (2008). Near-infrared emission from novel Tris (8-hydroxyquinolinate) lanthanide(III) complexes-functionalized mesoporous SBA-15. *Langmuir*, *24*, 5500–5507. DOI: 10.1021/la7036108.

Wang, Y., Li, B., Zhang, L., Liu, L., Zuo, Q., & Li, P. (2010). A highly selective regenerable optical sensor for detection of mercury(II) ion in water using organic–inorganic hybrid nanomaterials containing pyrene. *New Journal of Chemistry*, *34*, 1946–1953. DOI: 10.1039/c0nj00039f.

Xu, L., Xu, Y., Zhu, W., Yang, C., Han, L., & Qian, X. (2012). A highly selective and sensitive fluorescence "turn-on" probe for Ag^{+} in aqueous solution and live cells. *Dalton Transactions*, *41*, 7212–7217. DOI: 10.1039/c2dt30404j.

Xu, J., Hou, Y., Ma, Q., Wu, X., & Wei, X. (2013). A highly selective fluorescent sensor for Fe^{3+} based on covalently immobilized derivative of naphthalimide. *Spectrochimica Acta Part A: Molecular and Biomolecular Spectroscopy*, *112*, 116–124. DOI: 10.1016/j.saa.2013.04.044.

Xu, W., Zhou, Y., Huang, D., Su, M., Wang, K., & Hong, M. (2014). A highly sensitive and selective fluorescent sensor for detection of Al^{3+} using a europium(III) quinolinecarboxylate. *Inorganic chemistry*, *53*, 6497–6499. DOI: 10.1021/ic501010s.

Yadavi, M., Badiei, A., Ziarani, G., & Abbasi, A. (2013a). Synthesis of novel fluorene-functionalised nanoporous silica and its luminescence behaviour in acidic media. *Chemical Papers*, *67*, 751–758. DOI: 10.2478/s11696-013-0357-1.

Yadavi, M., Badiei, A., & Ziarani, G. M. (2013b). A novel Fe^{3+} ions chemosensor by covalent coupling fluorene onto the mono, di-and tri-ammonium functionalized nanoporous silica type SBA-15. *Applied Surface Science*, *279*, 121–128. DOI: 10.1016/j.apsusc.2013.04.048.

Zarabadi-Poor, P., Badiei, A., Yousefi, A. A., & Barroso-Flores, J. (2013). Selective optical sensing of Hg(II) in aqueous media by H-Acid/SBA-15: A combined experimental and theoretical study. *The Journal of Physical Chemistry C*, *117*, 9281–9289. DOI: 10.1021/jp401479z.

Zhao, Y., Lin, Z., Liao, H., Duan, C., & Meng, Q. (2006). A highly selective fluorescent chemosensor for Al^{3+} derivated from 8-hydroxyquinoline. *Inorganic Chemistry Communications*, *9*, 966–968. DOI: 10.1016/j.inoche.2006.05.030.

Zhou, X., Li, P., Shi, Z., Tang, X., Chen, C., & Liu, W. (2012). A highly selective fluorescent sensor for distinguishing cadmium from zinc ions based on a quinoline platform. *Inorganic chemistry*, *51*, 9226–9231. DOI: 10.1021/ic300661c.